

# RESEARCH

## Estimating Horizontal Dispersion of Floating Particles in Wind-driven Upper Ocean

MING LI\*

*Institute of Ocean Sciences, P.O. Box 6000, 9860 West Saanich Road, Sidney, B.C., Canada V8L 4B2*

Breaking waves and Langmuir circulation are dominant turbulent processes in a wind-driven upper ocean. Surface waves and, in particular, breaking waves can disintegrate an oil film, generating oil droplets or blobs of water-in-oil emulsions when the oil is weathered. Langmuir circulation, with its convergent and divergent flows at the ocean surface, can organize the floating particles into nearly parallel bands aligned in the wind direction. However, the rapid temporal evolution of the circulation makes it an effective mechanism for dispersing particles. In this paper, we estimate horizontal diffusivities of floating particles by examining Lagrangian particle statistics inferred from sonar images of the ocean surface. The diffusivities are in the range of  $O(10^{-3})$ – $O(1)$   $m^2 s^{-1}$  and depend on the crosswind and downwind velocities in Langmuir circulation. The particle dispersion on the ocean surface is not isotropic. The diffusivity in the crosswind direction is generally larger than that in the downwind direction. © 2001 Elsevier Science Ltd. All rights reserved.

**Keywords:** Turbulent dispersion, wind-driven upper ocean

### Introduction

When oil is spilled into the ocean, it forms a thin film of oil that spreads under the action of gravitational, viscous, and surface tension forces (Hoult, 1972). This early stage of oil spreading is usually short, lasting only for a couple of hours. At later stages, upper ocean processes dominate the oil spreading (and dispersion) unless wind is light (Galt, 1994). Small-scale ocean surface deformations associated with surface waves can rupture thin oil films so that they appear as streaks and streamers rather than as a continuous patch of pollutant. Breaking waves, which frequently occur in high-wind conditions, greatly facilitate the breakup of oil films and can generate oil droplets with radii of  $O(100)$   $\mu m$  or smaller (Li &

Garrett, 1998). As volatile oil components quickly evaporate, heavier oils begin to weather and form water-in-oil emulsions, or mousse. Wave action stretches and tears the weathered mousse into smaller blobs, ultimately down to small tarballs. Floating materials such as large oil droplets and emulsion blobs are advected and dispersed on the ocean surface by turbulent motions. Langmuir circulation is a dominant turbulent process in a wind-driven upper ocean (Langmuir, 1938). The circulation consists of counter-rotating vortices, thus generating divergent and convergent flows for floating particles. Figure 1 shows an aerial view of an oil spill in windy conditions. In both the bottom half of the oil patch and the arm extending in the top-left direction, the oil film is broken into many streaks roughly oriented in the wind direction.

Although the upper ocean processes clearly affect the distribution of oil on the ocean surface, their effects are not represented in oil spill trajectory models. Hydrodynamic models used for the oil-spill trajectory

\*Tel.: +1-250-363-6343; fax: +1-250-363-6746.

E-mail address: lim@pac.dfo-mpo.gc.ca (M. Li).



**Fig. 1** An aerial photograph of an oil spill. Oil streaks organized into roughly parallel bands oriented in the wind direction. Courtesy of National Oceanic and Atmospheric Administration's Hazardous Materials Response Division.

prediction have a coarse resolution of a few kilometers and employ depth-averaged shallow water equations to predict tides and storm surges (Elliot, 1991). To consider the effect of wind, a surface-drift current at approximately 3% of the wind speed is added to the particle advection. Turbulent processes are not resolved but instead are parameterized by an eddy diffusivity. The diffusivity is often chosen in order that the models reproduce known distributions of a released tracer. Hence, these models require tuning and may be of limited use in the actual prediction of spills (Turrell, 1994).

In this paper, we investigate dispersion of floating particles using sonar observations of upper ocean turbulent flow. Our objective is to provide an estimate (or a formula) of horizontal diffusivity that may be used in oil-spill trajectory models. Air bubbles generated by breaking waves are excellent acoustical targets and can be easily detected by sonar. Like oil droplets, these bubbles will also be collected at convergence zones of Langmuir circulation. Sonar images of bubble clouds thus provide maps of surface flow patterns. Tracking floating particles through the evolving flow patterns will give an idea how they congregate or disperse at the ocean surface. Because air bubbles and spilled oil organize into bands at convergence zones,

Langmuir circulation may appear to be a mechanism for concentrating particles. However, the circulation field rapidly evolves with time and this rapid temporal evolution makes Langmuir circulation an effective mechanism for horizontal dispersion.

## A Lagrangian Dispersion Model

This paper builds on previous observational and theoretical studies. Thorpe and Cure (1994) and Thorpe *et al.* (1994) used sonar observations to infer the surface dispersion of particles. They found that the crosswind diffusivity varies from  $5 \times 10^{-3}$  to  $0.5 \text{ m}^2 \text{ s}^{-1}$  and depends on the circulation lifetime,  $T_c$ , the mean wind drift,  $\bar{u}$ , and the velocity field of Langmuir circulation such as the crosswind velocity,  $v$ , and the excess downwind velocity,  $\Delta u$ , at the convergence lines (or the downwind jet strength). However, their sonars scanned the ocean surface in a fixed direction and could not directly measure the two-dimensional surface distributions of Langmuir convergence zones. Using a two-dimensional numerical model of Langmuir circulation, Colbo and Li (1999) investigated the dispersion of passive and buoyant particles in Langmuir circulation field and obtained a crosswind diffu-

sivity that is independent of eddy viscosity at high Reynolds numbers. However, their model cannot resolve three-dimensional flow patterns, which are important in high-wind conditions.

Using mechanically steered 100 kHz narrow-beam sidescan sonars, Farmer and Li (1995) obtained two-dimensional images of the ocean surface at about 40 s intervals (Fig. 2). The sonar instrument is suspended from a surface float by a rubber cord to 24 m depth and is therefore free to drift with the prevailing current. Bands of dark color, corresponding to high levels of sonar backscatter intensity, indicate the locations of high concentrations of bubbles or Langmuir convergence zones. Since the distribution of Langmuir convergence zones does not change much during 40 s period, their temporal evolution can be followed in the succession of images. For example, Farmer and Li (1995) tracked a Y-shaped junction over a 6 min period as it slowly moves and deforms. These images were processed to produce binary patterns of the convergence lines, shown as solid lines in Fig. 3. These convergence lines are generally oriented in the wind direction, though there is a wide range of line lengths

and spacings. Farmer and Li (1995) analyzed the distributions of windrow spacings and lengths and found that the average spacing between the lines shows a slight increase with increasing wind speed.

The skeletonized line patterns reveal information about the flow field of Langmuir circulation. A particle floating on the sea surface moves across the wind towards its nearest convergence line. Once it reaches the convergence line, it moves along that line until exiting from one end. Because there were no simultaneous measurements of the velocity field, a horizontal velocity field is prescribed according to the observed line pattern. As a simplification, we set the particle to move at a constant crosswind velocity,  $v$ . Because the instrument drifted with the prevailing current, it is assumed that no relative movement exists between the surface water and the instrument. Once a particle is trapped at a convergence line, it moves downwind at an excess speed,  $\Delta u$ , until it reaches the end of that line. A smaller-scale background diffusion, represented by a random walk with step size  $L = (4K_t\Delta t)^{1/2}$  is added to the horizontal advection of particles.

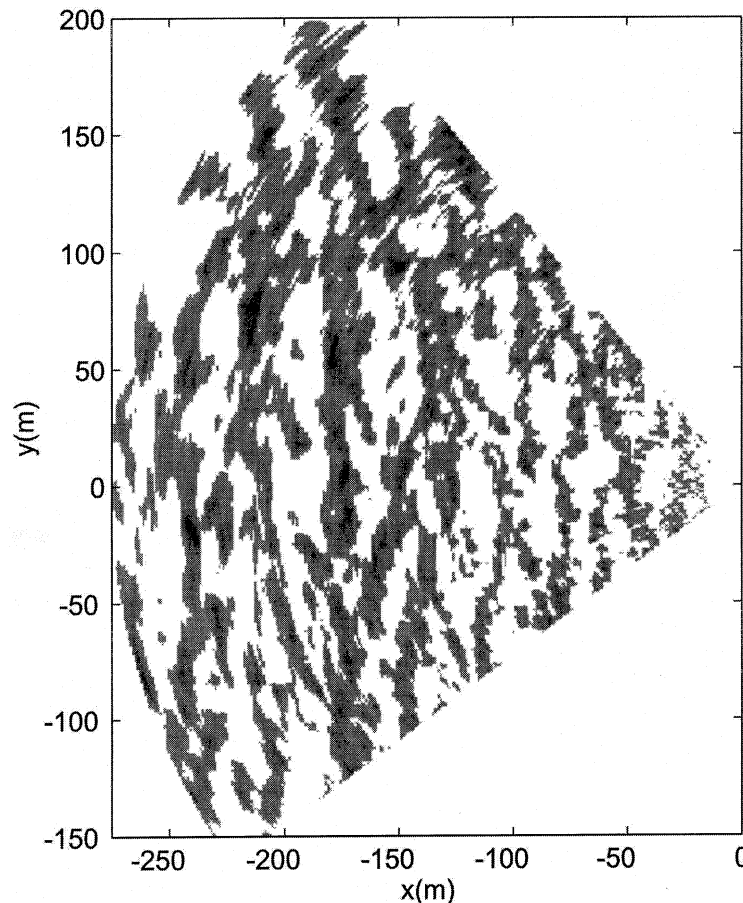


**Fig. 2** A two-dimensional sonar image of the ocean surface obtained during an experiment in the Strait of Georgia on the west coast of Canada. To emphasize the structure in this gray-scale image, we use a threshold below which the signal is shown as white.

Figure 3 shows the distributions of floating particles at the start of a dispersion experiment and at two subsequent times in 14 min intervals. In this experiment we seeded 121 particles in a rectangular area (Fig. 3(a)). The parameters are chosen to be  $v = \Delta u = 0.05 \text{ m s}^{-1}$  and  $K_t = 3 \times 10^{-3} \text{ m}^2 \text{ s}^{-1}$ . The particles move within a field of convergent and divergent flows. At about every 40 s, a new image and a corresponding flow field are used to drive the particle movement. By comparing particle distributions at different times (Figs. 3(b) & (c)), we notice that the particles have moved apart rather than have concentrated, confirming that Langmuir circulation is dispersive.

Taylor (1922) showed that in a stationary and homogeneous turbulence field, the variances  $\sigma_x^2$  and  $\sigma_y^2$  of particle displacement can be calculated from

$$\sigma_x^2(t) = 2\overline{u^2} \int_0^t (t - \tau)R_x(\tau) d\tau,$$

$$\sigma_y^2(t) = 2\overline{v^2} \int_0^t (t - \tau)R_y(\tau) d\tau,$$

where  $x$  is in the downwind direction,  $y$  is in the crosswind direction,  $\overline{u^2}$  and  $\overline{v^2}$  are the averaged velocity variances, and  $R_x$  and  $R_y$  are the velocity autocorrelation functions. Accordingly, the eddy diffusivities are given by

$$\kappa_x^2(t) = \overline{u^2} \int_0^t R_x(\tau) d\tau \Rightarrow \overline{u^2}T_x,$$

$$\kappa_y^2(t) = \overline{v^2} \int_0^t R_y(\tau) d\tau \Rightarrow \overline{v^2}T_y$$

as  $t \Rightarrow \infty$ . Thus the diffusivities at large times are products of turbulence intensity and Lagrangian decorrelation times  $T_x$  and  $T_y$ . The condition of stationarity and homogeneity is roughly satisfied in our model, since we consider a 1/2-h period during which the wind is approximately steady. Figures 4(a) & (b) shows the history of the two velocity components following a particle. In Fig. 4(a), the mean downwind velocity is subtracted from the time series. Figures 5(a) & (b) show the ensemble-averaged autocorrelation functions. Both functions show a rapid decay in time, with a Lagrangian decorrelation time in the range of a couple of minutes. Figure 6 shows the time series of the variances and eddy diffusivities for this experiment. At large times the variances increase linearly with time and the eddy diffusivities,  $\kappa_x(t)$  and  $\kappa_y(t)$ , approach their respective asymptotic limits,  $K_x$  and  $K_y$ .

### Estimates of Horizontal Diffusivities

We have run the dispersion experiments for various combinations of input parameters,  $K_t$ ,  $v$  and  $\Delta u$  in order to determine the functional dependence of eddy diffusivities,  $K_x$  and  $K_y$ , on these parameters. We considered both low and high-wind events. At low-wind conditions (wind speed less than  $10 \text{ m s}^{-1}$ ), convergence lines appeared to be regular, parallel lines oriented in the wind direction. At high-wind conditions (wind speed at  $13 \text{ m s}^{-1}$  or larger), convergence lines were less organized and some lines joined together to form Y-shaped junctions. Nevertheless, there were no significant differences in mean line spacings and lengths (Farmer and Li, 1995). We first test the sensitivity of eddy diffusivities to the background turbulent diffusivity,  $K_t$ . Table 1 summarizes the results. We observe no significant changes in  $K_x$  and  $K_y$

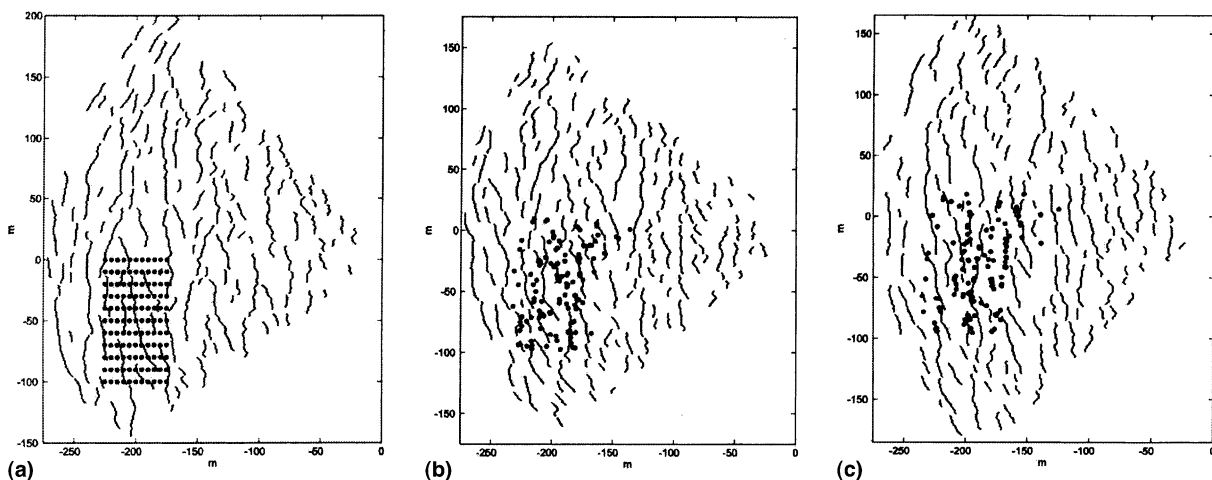


Fig. 3 Binary patterns of convergence lines obtained from the sonar images and the distribution of floating particles at three different times at Strait of Georgia on 24 November, 1991: (a) 10:22:34 PST; (b) 10:36:27 PST; (c) 10:50:01 PST.

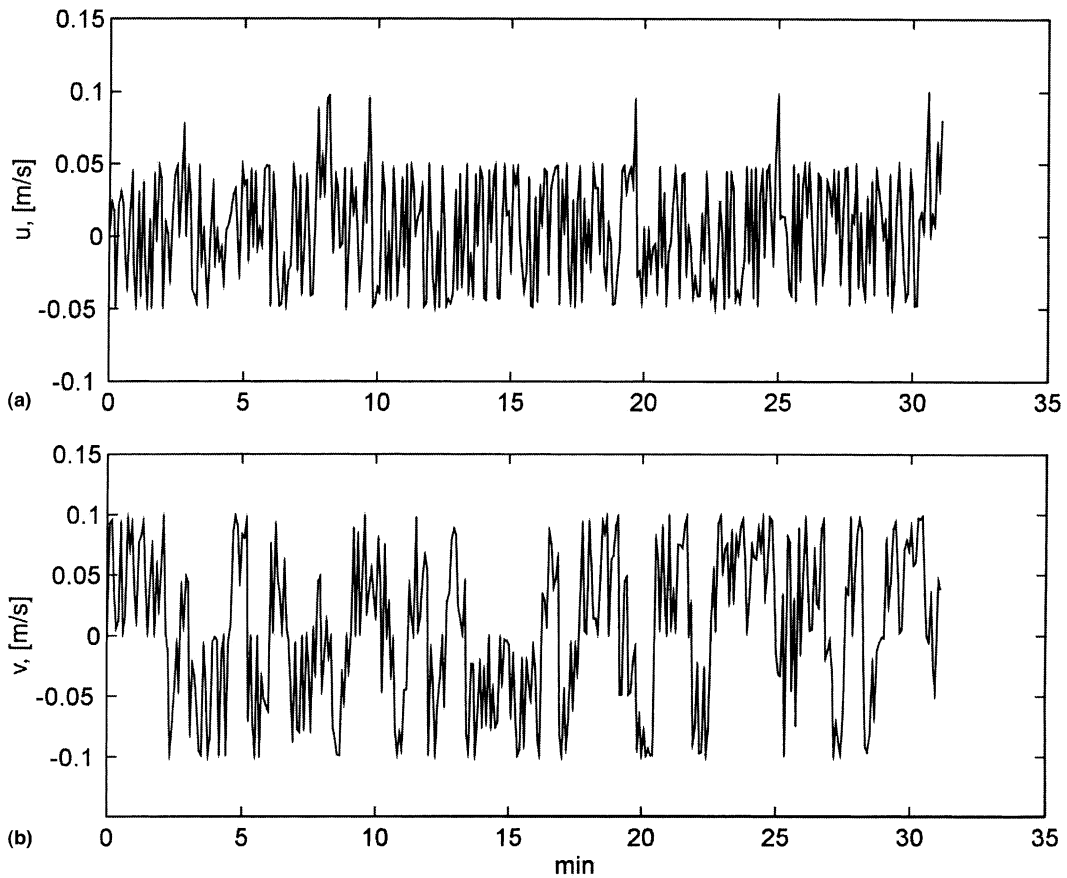


Fig. 4 Time series of downwind (minus the mean velocity) (a) and crosswind (b) velocity components following a particle.

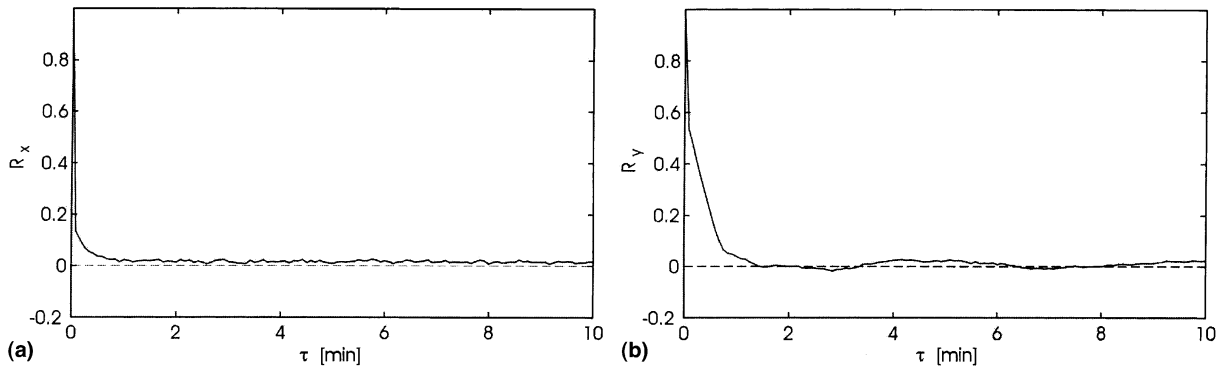


Fig. 5 Autocorrelation functions for the downwind (a) and crosswind (b) velocities.

at  $v = \Delta u = 0.05 \text{ m s}^{-1}$  and  $v = \Delta u = 0.1 \text{ m s}^{-1}$  as  $K_t$  varies over a wide range. Hence, the eddy diffusivities are insensitive to background diffusion. The movement of particles is determined mainly by the convergent-divergent motions of Langmuir circulation rather than by the background diffusion, even though the trajectory of a particle can become torturous at high values of  $K_t$ .

Secondly, we examine the dependence on the circulation velocities  $v$  and  $\Delta u$  over an observed range of

values. Figures 7 & 8 suggest no significant difference between the low- and high-wind periods, possibly because there were no significant changes in line spacings and lengths between the two periods. However, as shown in Fig. 7, both  $K_x$  and  $K_y$  show strong dependence on  $v$ . As  $v$  increases, particles spread apart faster in the crosswind direction so that  $K_y$  gets larger. Because particles can get to the convergence lines in shorter time, they spend relatively longer time moving along convergence lines so that  $K_x$  also increases with  $v$ .

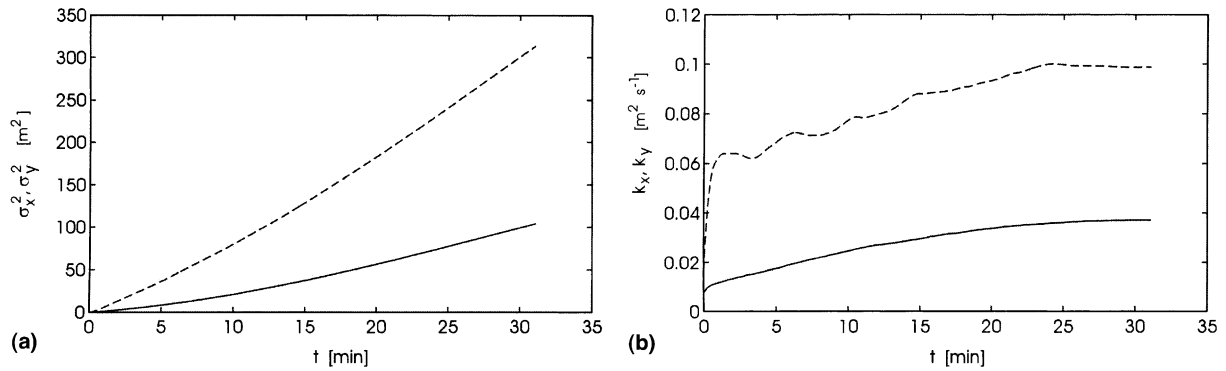


Fig. 6 Time series of variances (a) and horizontal diffusivities (b). Solid lines for the downwind components and dashed lines for the crosswind components.

Table 1 Sensitivity of downwind and crosswind diffusivities to the background diffusivity for two sets of Langmuir circulation velocities

$\Delta u = 0.05 \text{ m s}^{-1}, v = 0.05 \text{ m s}^{-1}$			
$K_t$ (m <sup>2</sup> s <sup>-1</sup> )	0	0.0001	0.003
$K_x$ (m <sup>2</sup> s <sup>-1</sup> )	0.037	0.035	0.037
$K_y$ (m <sup>2</sup> s <sup>-1</sup> )	0.1	0.09	0.1
$\Delta u = 0.1 \text{ m s}^{-1}, v = 0.1 \text{ m s}^{-1}$			
$K_t$ (m <sup>2</sup> s <sup>-1</sup> )	0	0.0001	0.01
$K_x$ (m <sup>2</sup> s <sup>-1</sup> )	0.78	0.80	0.62
$K_y$ (m <sup>2</sup> s <sup>-1</sup> )	0.62	0.64	0.67

Figure 8 shows how  $K_x$  and  $K_y$  vary with the downwind jet strength,  $\Delta u$ . The downwind diffusivity increases linearly with  $\Delta u$  whereas the crosswind component is insensitive to it. At larger values of  $\Delta u$ , particles can move longer distances along the convergence lines so that  $K_x$  increases with  $\Delta u$ . This however does not affect the movement of particles between the convergence lines in the crosswind direction. Generally, the circulation field depends not only

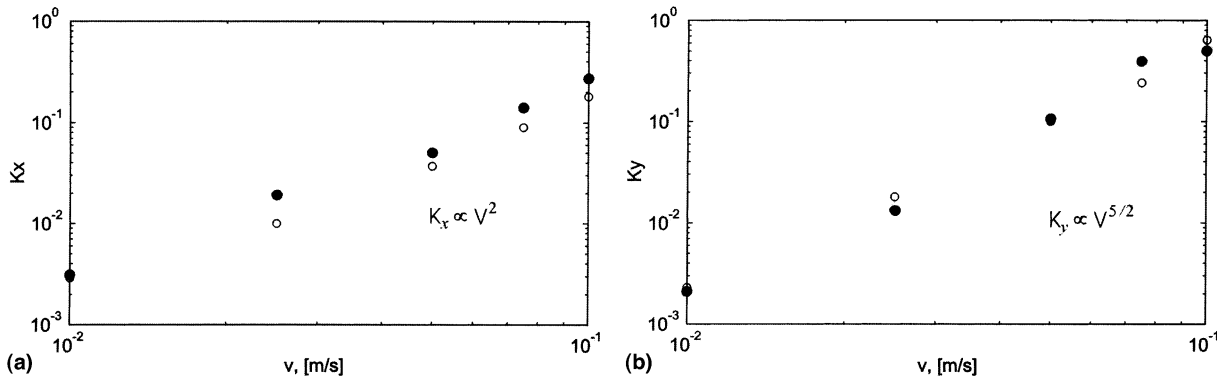


Fig. 7 Dependence of downwind (a) and crosswind (b) diffusivities on the crosswind velocity. Bullets represent data during the high-wind period and circles represent data from the low-wind period.

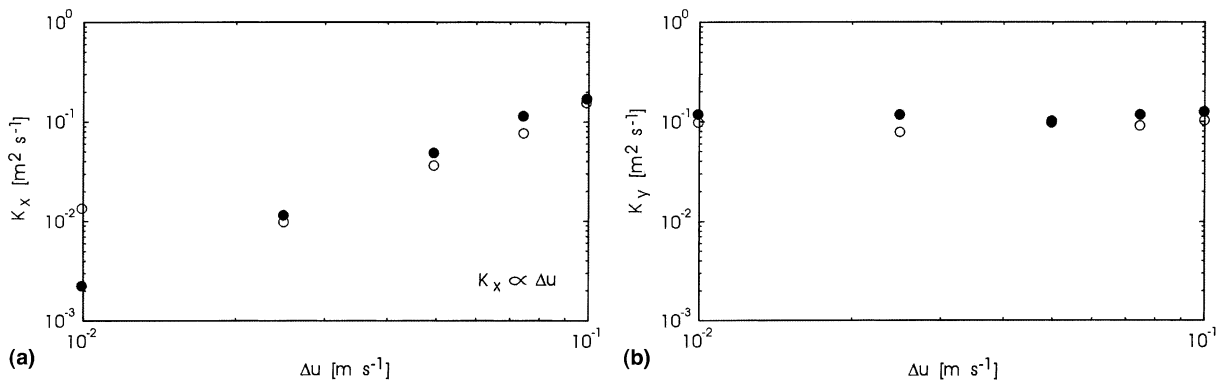


Fig. 8 Dependence of downwind (a) and crosswind (b) diffusivities on the downwind jet strength. Bullets represent data during the high-wind period and circles represent data from the low-wind period.

on the local wind speed but also on the wave field. For fully developed seas,  $v$  and  $\Delta u$  increase with the wind speed (Li and Garrett, 1993). Thus, both downwind and crosswind diffusivities will be larger at higher winds.

Comparing  $K_x$  and  $K_y$  in Figs. 7 & 8, we find that the crosswind diffusivity is generally larger than the downwind diffusivity. This non-isotropy in the horizontal diffusivity is related to different ways by which Langmuir circulation moves particles across the ocean surface. The particles move across the wind when lying between two adjacent convergence lines. They move downwind only when they are trapped at a convergence line. In general, particles spend more time moving between the convergence lines than along the convergence lines. Hence, Langmuir circulation is more effective in dispersing floating particles in the crosswind direction than in the downwind direction.

## Conclusion

Using sonar images of the ocean surface, we have carried out numerical experiments to study the horizontal dispersion of floating particles. We have obtained estimates of horizontal eddy diffusivities. Both  $K_x$  and  $K_y$  are in the range of  $O(10^{-3})$ – $O(1)$   $m^2 s^{-1}$ . These diffusivity values are smaller than the values of horizontal diffusivity used in larger-scale circulation models. It appears that mesoscale eddies and tidal residual flows may be more effective mechanisms for oil dispersion. Because the crosswind component  $K_y$  is generally greater than its downwind counterpart,  $K_x$ , an oil spill trajectory model may have to differentiate the crosswind and downwind diffusivities. Sensitivity studies show a strong dependence of the diffusivities on  $v$  and  $\Delta u$ . Because of this sensitivity, future simultaneous Doppler velocity measurements would be

very useful. Subject to further sensitivity tests for a wider range of sea conditions, the approximate power laws shown in Figs. 7 & 8 suggest that we may develop empirical formulae for the eddy diffusivities as functions of the wind speed and sea state. The formulae would provide a useful guide for choosing horizontal eddy diffusivities in operational oil spill models.

**Acknowledgements**—I am grateful to Chris Garrett, Keir Colbo and David Farmer for interesting discussions and one referee for perceptive comments. I thank Debra Simecek-Beatty, Bill Lehr, and Jerry Galt at the National Oceanic and Atmospheric Administration's Hazardous Materials Response Division for inviting me to attend the workshop on Langmuir circulation and oil spill modeling. This work was supported by a Canadian Natural Sciences and Engineering Research Council strategic grant.

## References

- Colbo, K., Li, M., 1999. Parameterizing particle dispersion in Langmuir circulation. *J. Geophys. Res.* 104, 26059–26068.
- Elliot, A.J., 1991. EUROSPELL: Oceanographical processes and NW European shelf databases. *Mar. Pollut. Bull.* 22, 548–553.
- Farmer, D.M., Li, M., 1995. Patterns of bubble clouds organized by Langmuir circulation. *J. Phys. Oceanography* 25, 1426–1440.
- Galt, J.A., 1994. Trajectory analysis for oil spills. *J. Adv. Mar. Technol. Conf. (JAMTEC)* 11, 91–126.
- Hoult, D.P., 1972. Oil spreading on the sea. *Ann. Rev. Fluid Mech.* 4, 341–368.
- Langmuir, I., 1938. Surface motion of water induced by wind. *Science* 87, 119–123.
- Li, M., Garrett, C., 1993. Cell merging and jet/downwelling ratio in Langmuir circulation. *J. Mar. Res.* 51, 737–769.
- Li, M., Garrett, C., 1998. The relationship between oil droplet size and upper ocean turbulence. *Mar. Pollut. Bull.* 36, 961–970.
- Taylor, G.I., 1922. Diffusion by continuous movements. *Proc. Lond. Math. Soc. Ser. A* 20, 196–211.
- Thorpe, S.A., Cure, M.S., 1994. One-dimensional dispersion in a lake inferred from sonar observations. In: Bevan, K.J., Chatwin, P.C., Millbank, J.H. (Eds.), *Mixing and Transport in the Environment*, pp. 17–28.
- Thorpe, S.A., Cure, M.S., Graham, A., 1994. Sonar observations of Langmuir circulation and estimation of dispersion of floating particles. *J. Atmos. Ocean Technol.* 11, 1273–1294.
- Turrell, W.R., 1994. Modelling the *Braer* oil spill. *Mar. Pollut. Bull.* 28, 211–218.